Environmental Pollution 230 (2017) 444–452

Contents lists available at ScienceDirect

Environmental Pollution

journal homepage: www.elsevier.com/locate/envpol

Air–sea exchange and gas–particle partitioning of polycyclic aromatic hydrocarbons over the northwestern Pacific Ocean: Role of East Asian continental outflow☆

Zilan Wu [a], Tian Lin [b, *], Zhongxia Li [a], Yuqing Jiang [a], Yuanyuan Li [a], Xiaohong Yao [c], Huiwang Gao [c], Zhigang Guo [a, **]

[a] Shanghai Key Laboratory of Atmospheric Particle Pollution and Prevention, Institute of Atmospheric Sciences, Department of Environmental Science and Engineering, Fudan University, Shanghai 200433, China
[b] State Key Laboratory of Environmental Geochemistry, Institute of Geochemistry, Chinese Academy of Sciences, Guiyang 550081, China
[c] College of Environmental Science & Engineering, Ocean University of China, Qingdao 266100, China

ARTICLE INFO

Article history:
Received 27 March 2017
Received in revised form
7 June 2017
Accepted 24 June 2017
Available online 1 July 2017

Keywords:
PAHs
Air–sea exchange
Gas–particle partitioning
East Asian continental outflow
Northwestern Pacific Ocean

ABSTRACT

We measured 15 parent polycyclic aromatic hydrocarbons (PAHs) in atmosphere and water during a research cruise from the East China Sea (ECS) to the northwestern Pacific Ocean (NWP) in the spring of 2015 to investigate the occurrence, air–sea gas exchange, and gas–particle partitioning of PAHs with a particular focus on the influence of East Asian continental outflow. The gaseous PAH composition and identification of sources were consistent with PAHs from the upwind area, indicating that the gaseous PAHs (three-to five-ring PAHs) were influenced by upwind land pollution. In addition, air–sea exchange fluxes of gaseous PAHs were estimated to be −54.2–107.4 ng m^{-2} d^{-1}, and was indicative of variations of land-based PAH inputs. The logarithmic gas–particle partition coefficient ($\log K_p$) of PAHs regressed linearly against the logarithmic subcooled liquid vapor pressure ($\log P_L^0$), with a slope of −0.25. This was significantly larger than the theoretical value (−1), implying disequilibrium between the gaseous and particulate PAHs over the NWP. The non-equilibrium of PAH gas–particle partitioning was shielded from the volatilization of three-ring gaseous PAHs from seawater and lower soot concentrations in particular when the oceanic air masses prevailed. Modeling PAH absorption into organic matter and adsorption onto soot carbon revealed that the status of PAH gas–particle partitioning deviated more from the modeling K_p for oceanic air masses than those for continental air masses, which coincided with higher volatilization of three-ring PAHs and confirmed the influence of air–sea exchange. Meanwhile, significant linear regressions between $\log K_p$ and $\log K_{oa}$ ($\log K_{sa}$) for PAHs were observed for continental air masses, suggesting the dominant effect of East Asian continental outflow on atmospheric PAHs over the NWP during the sampling campaign.

1. Introduction

East Asia has experienced rapid industrialization and urbanization, as well as abundant anthropogenic activity. As such, it has been recognized as the predominant emitter of primary aerosols to the northwestern Pacific Ocean (NWP) (Kunwar et al., 2016). The atmospheric circulation of East Asia is dominated by the monsoon system, characterized by the northerly continental air mass in winter, which shifts seasonally to the prevailing ocean-oriented southerlies in summer (Ding, 1994). Under such conditions, the NWP is prone to receive aerosols via the dominant westerly winds from the surrounding land from mid-autumn to mid-spring (Kawamura et al., 2003; Lin et al., 2011). Studies have reported on the inter-annual and seasonal variations (Liu et al., 2003; Cheng et al., 2016), budgets (Bey et al., 2001), characteristics, and evolution of various substances and chemicals in the outflow region of East Asia (Russo et al., 2003; Matsui et al., 2013; Boreddy and Kawamura, 2015; Verma et al., 2015). However, these studies are mainly model-based or rely on ground measurements at remote

☆ This paper has been recommended for acceptance by Dr. Chen Da.
* Corresponding author.
** Corresponding author.
E-mail addresses: lintian@vip.gyig.ac.cn (T. Lin), guozgg@fudan.edu.cn (Z. Guo).

http://dx.doi.org/10.1016/j.envpol.2017.06.079
0269-7491/

fixed-point monitoring sites and concentrate on inorganic ions or species (Tang et al., 2004; Boreddy et al., 2014; Kunwar and Kawamura, 2014).

To contribute to our understanding of the export of East Asian emissions and subsequent impacts, additional research is needed on different types of compounds as novel means of quantification. In this study, we used PAHs as a tracer to elucidate the influence of continental outflow to the NWP via long-range atmospheric transport (LRAT). PAHs are semivolatile organic compounds from anthropogenic and natural sources that pose an environmental concern due to their potential toxicity to ecosystems and humans (Hoffman et al., 1984). In addition, numerous studies have examined their chemical properties related to environmental persistence and long-range transport. The semivolatility of PAHs suggests two possible major processes of environmental cycling: gas–particle partitioning in air (Lohmann and Lammel, 2004) and revolatilization from ground and water surfaces (Wania and Mackay, 1993; Semeena and Lammel, 2005). PAHs are partitioned in both the gas and particle phases, and influential factors include ambient temperature, aerosol characteristics, and interactions between aerosols and sorbed chemicals (Pankow, 1994; Lohmann et al., 2000). Further, gas–particle partitioning processes include organic matrix absorption and particle surface adsorption (Pankow, 1994; Finizio et al., 1997; Harner and Bidleman, 1998). Effects of source-dependent aerosol type on PAH partition coefficients have been observed (Harner and Bidleman, 1998), and the properties of particles affected by land can be used to determine the spatial distributions of gas–particle partitioning of pollutants (Gustafson and Dickhut, 1997). The application of organic aerosol-associated absorptive and adsorptive mechanisms of PAHs to atmosphere has been evaluated extensively, especially in heavily impacted source regions (Simcik et al., 1998; Lohmann et al., 2000; Odabasi et al., 2006). Guazzotti et al. (2003) found that up to 75% of carbon-containing particles in downwind marine atmosphere originated from land-based combustion and the strong affinity between PAHs and soot carbon. Thus, its influence on atmospheric PAH distribution, has been evaluated using soot–air partitioning in an adsorption model, in remote regions. Fernández et al. (2002) reported the importance of soot in atmospheric PAH distribution in continental background areas and reflected on the significance of the long-range transportation of soot particles. For gas exchange at the air-sea interface, Gonzalez-Gaya et al. (2016) presented the global air–sea exchange of PAHs, which revealed a larger net atmospheric input supported by land. This was in agreement with a scenario in the tropical Atlantic Ocean, where the air–sea exchange of PAHs was dominated by deposition from primary sources (Lohmann et al., 2013). However, surface seawaters could serve as a buffer and re-supply chemicals back into the boundary atmosphere when a reduction in source emissions occurs (Nizzetto et al., 2010). The transition of air–sea exchange from deposition to volatilization has been detected for several individual PAHs in the Mediterranean Sea (Mulder et al., 2014; Lammel et al., 2016), highlighting the interaction between ongoing continental emissions and secondary release from seawater. However, it is still unclear whether the distribution and fate of atmospheric PAHs over remote oceanic areas are consistent with the dual sorption processes of carbonaceous particles. In particular, it is unknown when remote oceanic areas are characterized by strongly sustained transport of carbonaceous particles from continental outflow and significant volatilization of PAHs from surface seawater, exactly as the atmospheric PAHs from the ECS (East China Sea) to the NWP.

The objectives of this study were to reveal the spatial distribution of PAHs influenced by air–sea exchange and gas–particle partitioning in the atmosphere, and to assess the role of the continental outflow on the basis of the mutual relationship between air–sea exchange and gas–particle partitioning during March 29 to May 6, 2015 along a west-to-east transect from the ECS to the NWP.

2. Materials and methods

2.1. Sampling

Air and seawater samples were collected from the ECS to the NWP covering an area of 25°N to 38°N in latitude and 120°E to 152°E in longitude on board the research vessel Dong Fang Hong 2 of the Ocean University of China (Fig. 1). Air samples (ca. 412 m^3) were collected via a high-volume air sampler operated at a constant flow rate of 300 L min^{-1} (Guangzhou Mingye Technology Co. Guangzhou, China). The sampler was placed windward on the upper-most deck of the ship to avoid possible contamination from the ship's exhausts and cut off power when the ship stopped. The sampler was equipped with a quartz fiber filter (QFF) held in a metal frame (20 × 25 cm; Pall Gelman, Port Washington, NY, USA) to separate airborne particles from the air stream, followed by a polyurethane foam (PUF) plug (6.5 cm in diameter, 7.5 cm in thickness, density 0.030 g cm^{-3}) placed in a glass holder to collect species in the gas phase. Field blank samples were obtained by exposing to air for only a few seconds. The QFF filters were conditioned in a dry box (maintained at 20 °C and 40% relative humidity) before and after sampling to calculate the mass of total suspended particles (see supporting information (SI) Text 2.1 for additional details).

Surface seawater samples (60–100 L/sample) were collected using a seawater-rinsed metal bucket. Particle-bound analytes were captured on a pre-combusted glass fiber filter (142 mm in diameter, bore size 0.7 μm; Whatman, Maidstone, UK) placed in a stainless steel filter holder, while dissolved PAHs were subsequently adsorbed by passing the filtrate through a glass column (25 mm internal diameter, 200 mm in length) packed with Amberlite XAD-2 and XAD-4 resin (1:1 of total 30 g, Sigma-Aldrich, St. Louis, MO, USA) using a peristaltic pump (see SI Text 2.1). In situ meteorology and hydrology data, including wind speed, air and water temperature, and salinity, were also obtained (SI Table S1 and Table S2).

2.2. Sample processing and analytical procedure

The PUF plugs and filters spiked with surrogate recovery standards (Ace-d_{10}, Phe-d_{10}, Chr-d_{12}, and Per-d_{12}) were Soxhlet-extracted with dichloromethane (DCM) for 48 h. The extract was concentrated by rotary evaporation and solvent-exchanged to n-hexane, and further reduced with a highly purified N_2. The clean-up and fractionation were performed on a 8 mm i.d. silica/alumina column, packed from the bottom to top, with neutral alumina (3 cm, 3% deactivated), neutral silica gel (3 cm, 3% deactivated), and anhydrous sodium sulfate (1 cm). Elution of each XAD cartridge was performed with DCM, then ultrasonically extracted (three times) with three 100 mL aliquots of DCM in water bath. A total volume of 300 mL was concentrated and fractionated using the procedure described for air samples. Determination of PAHs was performed on an Agilent 7890A GC equipped with a capillary column (30 m × 0.25 mm × 0.25 μm DB5-MS) coupled to an Agilent 5975C MSD. The temperature of the oven was programmed as follows: initial temperature of 50 °C (8 min hold), then raised to 150 °C at 8 °C min^{-1} and held for 3 min and ramped to 290 at 3 °C min^{-1}, maintained for 20 min. The abbreviations of the 15 measured PAHs, along with the details of the sample processing and analyses are summarized in SI Text 2.2.

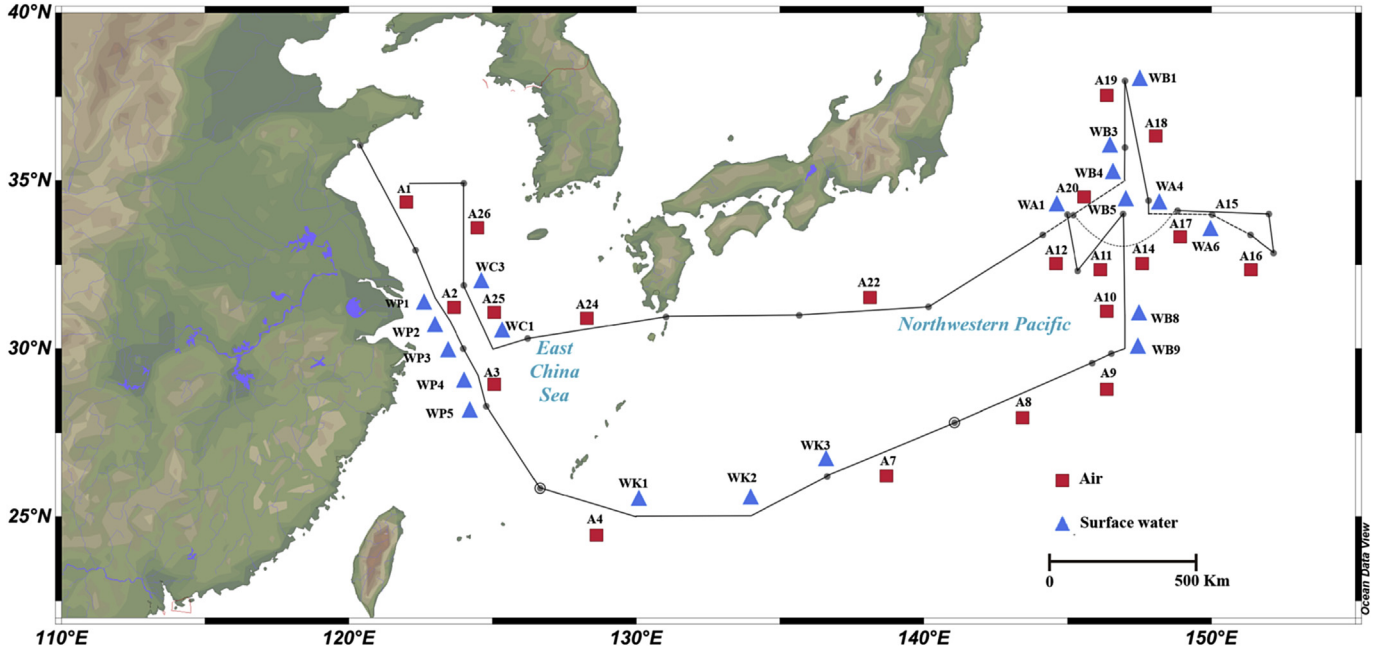

Fig. 1. Map of the cruise track of Dong Fang Hong 2, including the locations of seawater samples (blue triangles) and sampling transects of air samples (dotted lines). (For interpretation of the references to colour in this figure legend, the reader is referred to the web version of this article.)

2.3. Quality control and quality assurance

The quality control and assurance measures used during the experiment and collection processes are described in SI Text 2.3. Surrogate recoveries of air samples for Ace-d_{10}, Phe-d_{10}, Chr-d_{12}, and Per-d_{12} were 78 ± 6%, 94 ± 7%, 82 ± 9%, and 82 ± 7% in the gas phase, respectively, and 73 ± 8%, 88 ± 14%, 95± 10%, and 92 ± 13% in the particle phase, respectively. The recoveries of Ace-d_{10}, Phe-d_{10}, Chr-d_{12}, and Per-d_{12} in the water samples were 83 ± 15%, 93 ± 9%, 71 ± 8%, and 108 ± 13% in the dissolved phase, respectively, and 82 ± 10%, 96 ± 15%, 103 ± 15%, and 94 ± 12% in the water particulate phase, respectively. The method detection limits (MDLs), calculated as the mean field blank plus three times the standard deviation, were 0.019–0.35 pg m^{-3} for the air samples and 0.15–1.92 pg L^{-1} for the seawater samples. During the air sample collection, backup filters and split PUFs were applied. The subsequent analysis in our lab suggested filter adsorption bias and breakthrough loss as not interference with the gas–particle partitioning analysis, as the concentrations in the back-up absorbent or adsorbent were generally lower than the MDLs. Second XAD cartridges were applied to evaluate breakthrough during extraction of dissolved PAHs and no breakthrough of the target compounds was found.

2.4. Back trajectory analysis

To determine air mass origins for the cruise samples, five-day back trajectories (BTs) at 6-h intervals were computed in correspondence to each sampling episode by the HYSPLIT transport and dispersion model (http://ready.arl.noaa.gov/hysplit-bin/trajasrc.pl). Trajectories in coordinated universal time (UTC) were traced at 700 m above sea level.

2.5. Air-sea exchange

Diffusive air-sea exchange was quantitatively estimated by means of the widely applied Whitman two-film resistance model (Schwarzenbach et al., 2003). The flux of PAHs across the air-sea interface is a function of mass transfer coefficient and the concentration gradient between the truly dissolved and gas phase PAHs and is given by

$$F = k_{ol}\left(C_d - \frac{C_a}{H\prime}\right) \quad (1)$$

where k_{ol} (m d^{-1}) is the overall mass transfer coefficient, C_d (ng m^{-3}) is dissolved concentrations that deducted the dissolved organic carbon-sorbed portion, and C_a (ng m^{-3}) is the gas phase concentrations divided by the dimensionless Henry's law constant (H′).

k_{ol} is comprised of resistances to mass transfer through both water (k_w) and air layer film (k_a) and defined as

$$\frac{1}{k_{ol}} = \frac{1}{k_w} + \frac{1}{k_a H\prime} \quad (2)$$

where k_w and k_a are empirically obtained based on correlations with the wind velocity at a reference height of 10 m and the compound-specific molecular diffusivity. The temperature- and salinity-corrected H′and the concrete calculation of k_{ol} are given in SI Text 2.5.

3. Results and discussion

3.1. Occurrence of PAHs in the atmosphere

The sum of the 15 PAH concentrations (denoted hereafter as $\sum_{15}$PAHs), including both the gas and aerosol phases, in atmosphere were in the range of 3.9–13.8 ng m^{-3}, with a mean of 7.8 ng m^{-3} (Fig. S1). As summarized in Table 1, gaseous $\sum_{15}$PAHs dominated (3.6–13.6 ng m^{-3}), contributing 95.8± 2.1% to the total PAH concentrations. Compared with the available literature on the

Table 1
Summary of PAHs in atmosphere (gas and aerosol phase) and seawater samples (dissolved and particulate phase) collected from the ECS to the NWP.

Compound	Gas phase (ng m^{-3})		Aerosol phase (ng m^{-3})		Dissolved phase (ng L^{-1})		Particulate phase (ng L^{-1})	
	Mean (SD)	Range	Mean (SD)	Range	Mean (SD)	Range	Mean (SD)	Range
Acy	0.092 (0.17)	0.0055–0.65	0.0071 (0.0024)	0.0044–0.012	0.23 (0.063)	0.15–0.36	0.0055 (0.0081)	0.00035–0.022
Ace	0.22 (0.14)	0.084–0.65	0.035 (0.019)	0.018–0.084	1.3 (0.28)	0.76–1.9	0.0099 (0.012)	0.00073–0.039
Fl	1.0 (0.91)	0.25–3.1	0.061 (0.016)	0.043–0.089	2.4 (0.48)	1.5–3.6	0.042 (0.064)	0.00096–0.20
Phe	4.7 (1.9)	2.2–9.5	0.060 (0.0098)	0.043–0.085	3.7 (1.3)	1.7–7.6	0.043 (0.075)	0.0056–0.31
Ant	0.36 (0.21)	0.10–0.73	0.0062 (0.0018)	0.0033–0.0094	0.62 (0.15)	0.40–1.0	0.0085 (0.018)	0.00039–0.074
Flu	0.55 (0.27)	0.23–1.1	0.016 (0.016)	0.0054–0.076	0.48 (0.22)	0.30–1.1	0.0041 (0.0039)	0.00096–0.013
Pyr	0.41 (0.33)	0.14–1.7	0.026 (0.012)	0.0096–0.058	0.30 (0.24)	0.10–1.2	0.0030 (0.0026)	0.00086–0.011
BaA	0.015 (0.015)	0.0011–0.052	0.0044 (0.0028)	0.0015–0.011	0.028 (0.041)	0.010–0.19	0.0010 (0.0012)	0.00023–0.0051
Chr	0.095 (0.10)	0.031–0.45	0.017 (0.013)	0.0039–0.052	0.17 (0.30)	0.037–1.4	0.0019 (0.0021)	0.00039–0.0091
BbF	0.021 (0.015)	0.0047–0.063	0.016 (0.019)	0.0015–0.073	0.012 (0.012)	0.0019–0.050	0.014 (0.012)	0.0034–0.054
BkF	0.0042 (0.0023)	0.0013–0.0080	0.0065 (0.0055)	0.00044–0.019	0.013 (0.013)	0.0020–0.044	0.0020 (0.0025)	0.00039–0.012
BaP	0.0021 (0.0022)	0.00054–0.011	0.0032 (0.0044)	nd–0.017	0.011 (0.0072)	nd–0.028	0.0011 (0.0015)	0.00017–0.0067
IcdP	0.0033 (0.0034)	0.00014–0.015	0.0077 (0.010)	nd–0.038	0.011 (0.0049)	0.0035–0.021	0.0014 (0.0018)	0.00032–0.0080
DahA	0.00010 (0.00039)	nd–0.0018	0.0011 (0.0030)	nd–0.011	0.046 (0.047)	0.0079–0.16	0.00063 (0.00075)	nd–0.0026
BghiP	0.0031 (0.0031)	0.00039–0.014	0.0074 (0.0092)	nd–0.030	0.0070 (0.0051)	nd–0.016	0.0015 (0.0019)	0.00028–0.0083
$\sum_{15}$PAHs	7.5 (3.2)	3.6–13.6	0.27 (0.090)	0.17–0.55	9.3 (2.4)	5.5–15.5	0.14 (0.17)	0.024–0.69

nd: not detected.

north Pacific Ocean, the total PAH concentrations (gas + aerosol) in the NWP in this study were lower than those reported by Ding et al. (2007) and Gonzalez-Gaya et al. (2016), but higher than those of Ma et al. (2013). In comparison with other studies, our results were lower than samples collected in the northeast subtropical Atlantic atmosphere (Del Vento and Dachs, 2007). Gaseous levels of $\sum_{15}$PAHs in our study were below those reported in the Asian marginal seas and the Indian Ocean, while the aerosol phase concentrations were comparable (Xu et al., 2012). The overwhelming contribution of gaseous $\sum_{15}$PAHs compared with particulate $\sum_{15}$PAHs in this study was consistent with the removal of particle-bound PAHs in the transport pathway from the continent to the open ocean (Xu et al., 2012; Ma et al., 2013). It should not be surprising that our results differed from those observed in near-shore atmospheres, where a higher proportion of particulate PAHs were measured (Kim et al., 2012; Wang et al., 2014)

There was nearly a four-fold variation in gaseous $\sum_{15}$PAHs during the sampling campaign (Fig. S1). Higher values of gaseous $\sum_{15}$PAHs (e.g., at sites A2 and A3) were generally observed in the atmosphere over areas closer to the coast affected by land-derived emissions. High values of gaseous $\sum_{15}$PAHs were also measured in air samples A15, A17, and A20, representative of the remote marine atmosphere. The sampling campaign was carried out in mid-spring, when the air circulation was dominated by westerly winds. The back trajectories shown in Figure S2 indicated that most of the continental air masses during the cruise traveled across the north and east of China, occasionally sweeping along the Korean Peninsula and Japan. This indicated that the atmosphere at the relatively distant sites still received significant inputs of East Asian land-derived PAHs, which was related to the strong continental outflow. The East Asian monsoon acts as a carrier of upwind pollutants, greatly influencing the atmospheric conditions in the downwind regions (Bey et al., 2001; Liu et al., 2003; Russo et al., 2003). To expand our understanding of possible factors associated with the spatial distribution of gaseous PAHs in addition to the origin of the air mass, we plotted the partial pressure in the natural logarithm lnP (Pa) against the inverse of ambient temperature 1/T (K^{-1}) (Fig. S3). There was no significant correlation between the gaseous PAHs and temperature, possibly due to the narrow temperature range (18.72 ± 3.25 °C) during the sampling period, supporting the source-dependent spatial difference in PAHs over the NWP due to LRAT.

The atmospheric PAH composition profiles among the sampling sites were statistically similar ($R^2 = 0.90–0.99$, $P < 0.05$), implying similar sources, despite the large variation of concentrations of these chemicals. The ratios of Flu/(Flu + Pyr) and IcdP/(IcdP + BghiP) were in range of 0.33–0.67 and 0.37–0.59, respectively (Fig. S4), indicative of pyrogenic origins of either petroleum and coal combustion or biomass burning. Therefore, land-derived PAHs from pyrogenic processes from upwind of the NWP governed the PAH profiles over the study area.

3.2. Air–sea gas exchange of PAHs

The $\sum_{15}$PAH concentrations in seawater (dissolved + particulate) ranged from 5.5 to 15.6 ng L^{-1}, with a mean of 9.4 ng L^{-1} (Fig. S5). Compared with dissolved PAH levels collected during a cruise surveillance of the East and South China Seas (Ren et al., 2010), our values were generally lower. However, the PAH concentrations in this study were substantially higher than those measured in the North Pacific, Arctic (Ma et al., 2013; Gonzalez-Gaya et al., 2016), and Atlantic Oceans (Nizzetto et al., 2008).

The $\sum_{15}$PAH fluxes varied on a spatial scale, ranging from −54.2–107.4 ng m^{-2} d^{-1}. The net deposition in the marginal sea (i.e., P4 and P5) was consistent with the co-influence of proximity to land and continental air masses. The air–sea exchange of the $\sum_{15}$PAHs revealed net volatilization in the open ocean except a relatively remote site A6. The net deposition of $\sum_{15}$PAHs observed at site A6 was a reflection of high gaseous PAH concentrations to low dissolved PAHs in seawater owing to the strong input from the continental outflow. The three-ring PAHs with larger Henry's law constants were prone to undergo volatilization (or near equilibrium conditions) due to their fugacity gradients at the air–sea interface and inherent compound-specific properties (Table S3). The net exchange fluxes of the three-ring PAHs ranged from 25.0 to 161.4 ng m^{-2} d^{-1}. The magnitudes of volatilization fluxes for three-ring PAHs in the study area were impeded by increasing concentrations of gaseous PAHs when the influence from continental outflow enhanced. Conversely, the higher volatilization found in the open ocean was the result of oversaturation of dissolved PAHs to upper atmospheric ones when the influence from continental outflow weakened. (Fig. 2). However, sites C1 and C3 in the marginal sea displayed substantial volatilization of three-ring PAHs.

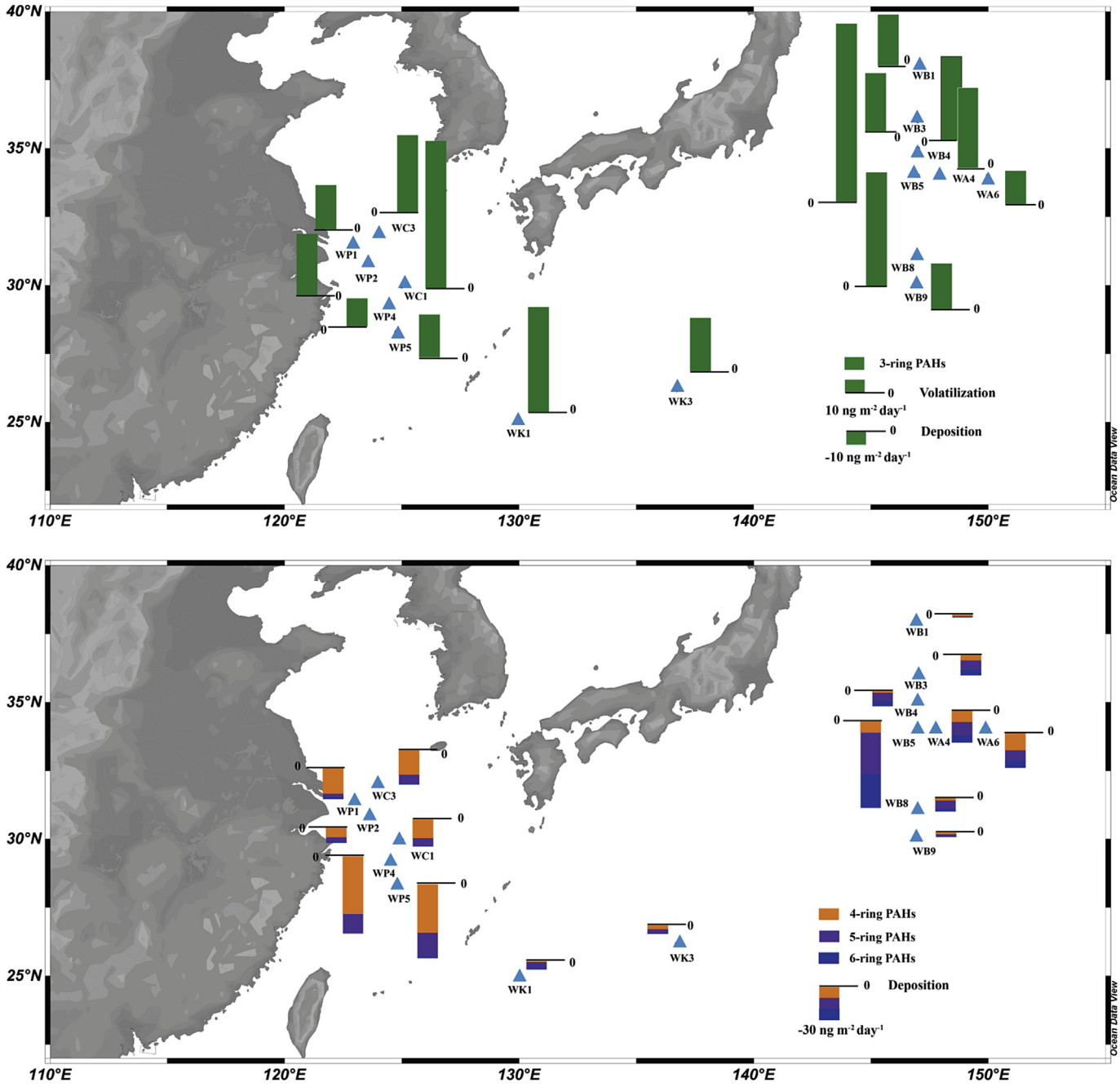

Fig. 2. Air–sea exchange fluxes of three-ring PAHs (upper panel) and four-to six-ring PAHs (lower panel). Positive flux (greater than 0) indicates volatilization.

This spatial inconsistency was due to low gaseous PAH concentrations and high dissolved PAHs in seawater. These air samples were collected in May; the wind circulation pattern after May exhibited an occasional shift, with winds beginning to come from the Pacific (Verma et al., 2015) thereby restricting inputs of land-derived PAHs under the influence of oceanic air masses delivered by the easterlies. Therefore, gaseous exchange processes of the three-ring PAHs at the air–sea interface could be the result of land-based inputs and release from local surface seawater. In addition, there was a positive relationship between the exchange fluxes of three-ring PAHs and wind speeds ($R^2 = 0.53$ and $P < 0.01$, Fig. S6), indicating that the transfer of three-ring PAHs via volatilization from the surface seawater was facilitated by wind speed, especially in highly windy remote areas.

The gas phase Phe had an exclusive burden of 63.6± 7.5% followed by Fl (13.0± 7.7%) in the atmosphere from the ECS to the NWP. This composition was distinguished from the volatilization-dominated case, where an increase in gaseous concentrations was proportional to increasing molecular weight (Gigliotti et al., 2002), suggesting that Phe and Fl in the study area was mainly input from upwind emissions via LRAT. Furthermore, we assessed the relationship between the net flux and gas phase concentrations of the three-ring PAHs to clarify the effect of continental outflow (Fig. S7). Even though the three-ring PAHs were associated with

volatilization, no significant correlation was observed between volatilization fluxes and gaseous concentrations, indicative of a less important secondary source from surface seawater.

Unlike the three-ring PAHs, deposition of four to six-ring PAHs (−79.2 to −2.8 ng m^{-2} d^{-1}) occurred uniformly (Fig. 2). The observed deposition fluxes of four to six-ring PAHs were probably replenishments due to their low dissolved concentrations relative to those in gas phase counterparts. In general, the magnitudes of the gross four-ring PAH deposition fluxes were greater in the west marginal sea and decreased with distance from the coast (Fig. 2). The dilution effect and atmospheric dry deposition scavenging of these PAHs resulted in limited deposition in the open ocean. Meanwhile, notable deposition of five to six-ring PAHs was detected at the east-most areas of the NWP, which was possibly affected by vehicular exhaust and fossil fuel combustion emissions from Japan. Regarding the net depositional PAHs, the linear fitting of statistical significance revealed that the increasing deposition fluxes were accompanied with high levels of high molecular weight PAH in the gaseous phase (Fig. S7). These results were similar to scenarios in the North Pacific and Arctic Oceans (Ma et al., 2013), as well as the tropical Atlantic Ocean (Lohmann et al., 2013), with a net deposition, suggesting a dominant role of continental outflow in the oceanic atmosphere by LRAT.

3.3. Gas–particle partitioning and implications for the effects of continental outflow

The gas–particle partition coefficient (K_p) can be expressed as $C_p/(TSP \times C_g)$, where C_p and C_g are PAH concentrations in the aerosol and gas phases (ng m^{-3}), respectively, and TSP is the total suspended particle concentrations in the air (μg m^{-3}). Only PAH concentrations in both aerosol and gas phase above the detection limits are used to calculate K_p values. A linear relationship between $\log K_p$ and $\log P_L^0$ (i.e., vapor pressure of the subcooled liquid, P_L^0) was developed (Fig. 3), and the temperature-dependent P_L^0 of PAHs was adjusted based on the method of Lei et al. (2002).

$$\log k_p = m \log P_L^0 + b \quad (3)$$

The linear regression of $\log K_p$ against $\log P_L^0$ for 10 PAHs (i.e., Ace, Fl, Phe, Ant, Flu, Pyr, BaA, Chr, BbF and BkF) found in all samples was observed with a slope of −0.25 ($R^2 = 0.37$, $P < 0.001$). This slope deviated from −1, reflecting that the phase distribution was not at theoretical equilibrium, possibly because continentally derived PAHs contained more non-exchangeable PAHs (Pankow and Bidleman, 1991) and/or the diffusion and mixing processes of air masses underwent over the NWP. Besides, $\log K_p$ was significantly linearly correlated with the aerosol phase PAH concentrations (ng mg^{-1}), highlighting the importance of organic components of aerosol particles on K_p. (Fig. S8). In other words, the particle-bound PAHs played a dominant role in the determination of K_p in the sampling period. In particular, the role of soot adsorption in gas–particle partitioning in the remote marine atmosphere should be taken into account. Meanwhile, given the impact of sea-to-air release of gaseous PAHs and marine-derived OM on status of atmospheric gas–particle partitioning, we applied the partitioning model of Dachs and Eisenreich (2000), inclusive of both absorption and soot-induced adsorption processes to evaluate the potential factors on K_p values for PAHs, with the equation:

$$kp = f_{OM}\frac{\zeta_{OCT}}{\zeta_{OM}\rho_{OCT}}\frac{MW_{OCT}}{MW_{OM}10^{12}}K_{OA} + f_{EC}\frac{\partial_{EC}}{\partial_{AC}10^{12}}K_{SA} \quad (4)$$

where K_{oa} and K_{sa} are the octanol–air and the soot–air partition coefficients, f_{OM} and f_{EC} are the mass fractions of organic matter (OM) and elemental carbon (EC) in aerosols, respectively, ζ_{OCT} and ζ_{OM} are the activity coefficients in octanol and OM, respectively, MW_{OCT} and MW_{OM} are the molecular mass of octanol and OM, respectively, ρ_{OCT} is the density of octanol (0.82 kg L^{-1}), and ∂_{EC} and ∂_{AC} are specific surface areas of EC and activated carbon, respectively. The above equation was simplified by assigning MW_{OCT}/MW_{OM}, $\partial_{EC}/\partial_{AC}$, and ζ_{OCT}/ζ_{OM} as 1, a common assumption for this calculation (Dachs and Eisenreich, 2000; Fernández et al., 2002). The applied values and considerations of other parameters f_{OM}, f_{EC}, K_{oa} and K_{sa} were provided in SI text 2.6.

Overall, the modeling results showed that the predictions of four-ring PAHs (Flu, Pyr, and BaA) best approximated the field measurements, indicating that both adsorption and absorption processes exerted an influence on these PAHs in atmosphere (Fig. 4). Meanwhile, deviations existed for the other PAHs, with underestimations of 3.08 ± 0.41, 2.35 ± 0.43, and 0.85 ± 0.25 log units for the lighter Ace, Fl, and Phe, and overpredictions of 1.15 ± 0.51 and 0.80 ± 0.45 log units for the heavier BbF and BkF (see Fig. 4).

Discrepancies were observed under two different types of air masses based on the model results. As shown in Fig. 4, more positive and negative deviations were found for the three-ring and five-ring PAHs, respectively, in the oceanic air masses, compared to the K_p in the continental air masses which were more close to

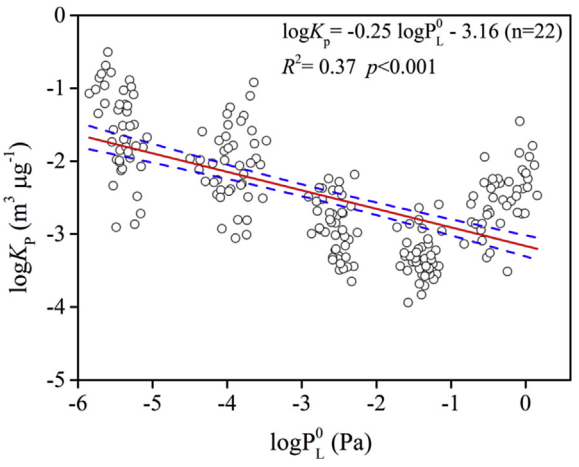

Fig. 3. Relationship between $\log K_p$ and temperature-corrected $\log P_L^0$.

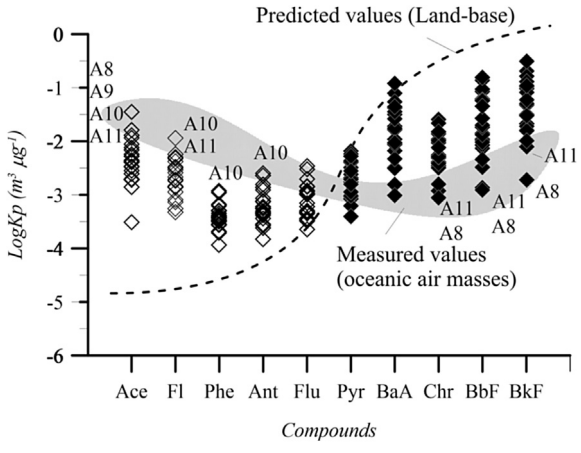

Fig. 4. Comparison of field-measured (diamond) and predicted (dotted curve) $\log K_P$ values of 10 PAHs considering both absorption and adsorption processes. The shaded area represents the oceanic air masses.

Table 2
Gas–particle partitioning of PAHs (mean ± SD), observed and predicted logK_p by the combined K_{oa}–K_{sa} model. Deviations (mean ± SD) of predicted values relative to observed logK_p for oceanic air masses (a) and continental air masses (b).

Compound	Observed		K_{oa}-K_{sa}		Deviation (a)		Deviation (b)	
	Mean	SD	Mean	SD	Mean	SD	Mean	SD
Ace	−2.30	0.35	−5.38	0.10	−3.62	0.19	−2.92	0.29
Fl	−2.64	0.37	−4.99	0.11	−2.83	0.13	−2.20	0.37
Phe	−3.39	0.20	−4.24	0.12	−1.02	0.17	−0.80	0.25
Ant	−3.23	0.33	−4.21	0.12	−1.11	0.36	−0.93	0.32
Flu	−3.13	0.33	−3.21	0.14	0.03	0.22	−0.11	0.32
Pyr	−2.68	0.34	−3.16	0.14	−0.48	0.25	−0.48	0.36
BaA	−1.88	0.55	−1.85	0.16	0.06	0.35	0.01	0.60
Chr	−2.26	0.38	−1.74	0.16	0.75	0.25	0.45	0.35
BbF	−1.78	0.58	−0.63	0.17	1.70	0.46	0.98	0.40
BkF	−1.44	0.52	−0.64	0.18	1.24	0.43	0.66	0.36

predictive K_p. The simulations deviated from the field measurements by 3.23 ± 0.45 and 1.47 ± 0.49 log units in the case of three-ring (Ace and Fl) and five-ring (BbF and BkF) PAHs, respectively, for air samples A7–A11 characterized by oceanic provenience, which were larger than samples under continental air masses (2.56 ± 0.49 and 0.82 ± 0.41 log units) (Table 2). As already suggested by the air–sea exchange, the open ocean was a secondary source of three-ring PAHs. Nonetheless, the K_p values in air samples A7–A11 were not reduced as followed by the new release of gaseous 3-ring PAHs and they exhibited enhancement instead. Released three-ring PAHs may sorb faster or be co-released with local OM-containing particles via sea spray bubbles from the surface seawater. Since phytoplankton activity flourished during the sampling period in the NWP (Obata et al., 1996), these results were in line with those of Cavalli et al. (2004), who found that the bubble bursting process contributed to the effective transfer of hydrophobic OM in surface seawater to marine aerosols during phytoplankton blooms. The relatively enhanced particulate proportions of three-ring PAHs possibly explained the higher K_p in the shift from continental air masses to oceanic air masses. As for the five-ring PAHs, the deviations were deemed to closely connect with a reduction in soot-phase concentrations. Five-ring PAHs of pyrogenic origin would be strongly sequestrated or irreversibly occluded in the soot matrix. The soot carbon fraction in aerosols would reduce over the course of the shift from continental air masses to oceanic air masses, which was indicated by the decrease in the ratio of soot carbon to fine particle carbon in the clean air masses (Andreae, 1983). During LRAT to the open NWP, soot-associated fractions may be partially recycled back into the water column by increased turbulence-driven dry deposition at high wind speeds (Jurado et al., 2004). The low content of soot in oceanic air masses was linked to decreased particle-associated fractions, resulting in lower field logK_p values compared to those in continental air masses. Thus, the non-equilibrium of PAH gas–particle partitioning could be shielded from the volatilization of three-ring gaseous PAHs from seawater and lower soot concentrations when oceanic air masses prevailed.

As discrepancies emerged in the samples of the two air mass types, the relationship between logK_p and logK_{oa} (logK_{sa}) was used as a descriptor to better understand the continental outflow strength (Fig. 5). A general trend was observed between the logK_p and logK_{oa} relationship (Fig. S9). The relationship tended to be more positive closer to land, and significant linear regressions were observed for samples with signals of land-based origins. In the case of the furthermost sites of the cruise (air samples A15–A18), strongly carbonaceous particles-dependent partitioning still appeared ($P = 0.006 \pm 0.009$, $R^2 = 0.53 \pm 0.10$), highlighting the predominant influence of East Asian continental outflow. East Asian continental outflow is a notable source of PAHs and organic aerosols especially soot particles over the ocean, and biomass burning, industrial emissions, and residential emissions via LRAT are considered to be major inputs. In comparison, insignificant relationships were found in oceanic air masses (Fig. S9), which may be partially influenced by the higher volatilization and lower soot-associated concentrations of PAH.

4. Conclusions

This study presents an extensive investigation of air–sea exchange and gas–particle partitioning of PAHs over the NWP for the first time and explores the interrelationships between them during LRAT. The transported PAHs mainly existed in gas phase in the study area. Higher concentrations were determined for samples proximity to the land and for periods with air masses of continental origin. The spatial variability of net air–sea exchange flux both in direction and magnitude was mainly influenced by the regional advective inputs of PAHs. As for the oceanic air masses, the volatilization of three-ring PAHs in gas phase at the air–sea interface and non-exchangeable fraction of PAHs contributed to the deviations from gas–particle partitioning equilibrium. Nonetheless, it should be pointed out that significantly linear regressions between logK_p and logK_{oa} (logK_{sa}) were indicative of the predominant

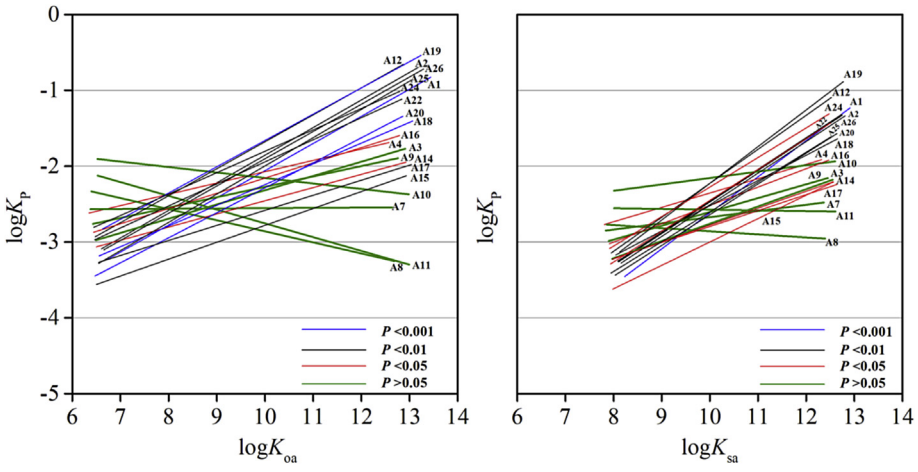

Fig. 5. Comparison of correlations between logK_p and logK_{oa} or logK_{sa} based on the statistical significance in atmosphere along the sampling track.

influence of East Asian continental outflow during the sampling campaign.

Acknowledgements

This work was supported by the National Basic Research Program of China (No: 2014CB953701) and Natural Science Foundation of China (NSFC) (Nos: 41376051, 41176085). We wish to thank the crew of R/V of Dong Fang Hong 2 of Ocean University of China for collecting samples. The anonymous reviewers should be sincerely appreciated for their constructive comments that greatly improved this work.

Appendix A. Supplementary data

Supplementary data related to this article can be found at http://dx.doi.org/10.1016/j.envpol.2017.06.079.

References

Andreae, M.O., 1983. Soot carbon and excess fine potassium: long-range transport of combustion-derived aerosols. Science 220, 1148–1151.

Bey, I., Jacob, D.J., Logan, J.A., Yantosca, R.M., 2001. Asian chemical outflow to the Pacific in spring: origins, pathways, and budgets. J. Geophys. Res. Atmos. 106, 23097–23113. http://dx.doi.org/10.1029/2001JD000806.

Boreddy, S.K.R., Kawamura, K., 2015. A 12-year observation of water-soluble ions in TSP aerosols collected at a remote marine location in the western North Pacific: an outflow region of Asian dust. Atmos. Chem. Phys. 15, 6437–6453.

Boreddy, S.K.R., Kawamura, K., Jung, J., 2014. Hygroscopic properties of particles nebulized from water extracts of aerosols collected at Chichijima Island in the western North Pacific: an outflow region of Asian dust. J. Geophys. Res. Atmos. 119, 167–178. http://dx.doi.org/10.1002/2013JD020626.

Cavalli, F., Facchini, M.C., Decesari, S., Mircea, M., Emblico, L., Fuzzi, S., Ceburnis, D., Yoon, Y.J., O'Dowd, C.D., Putaud, J.P., Dell'Acqua, A., 2004. Advances in characterization of size-resolved organic matter in marine aerosol over the North Atlantic. J. Geophys. Res. Atmos. 109, D24215. http://dx.doi.org/10.1029/2004JD005137.

Cheng, X., Zhao, T., Gong, S., Xu, X., Han, Y., Yin, Y., Tang, L., He, H., He, J., 2016. Implications of East Asian summer and winter monsoons for interannual aerosol variations over central-eastern China. Atmos. Environ. 129, 218–228.

Dachs, J., Eisenreich, S.J., 2000. Adsorption onto aerosol soot carbon dominates gas-particle partitioning of polycyclic aromatic hydrocarbons. Environ. Sci. Technol. 34, 3690–3697.

Del Vento, S., Dachs, J., 2007. Atmospheric occurrence and deposition of polycyclic aromatic hydrocarbons in the northeast tropical and subtropical Atlantic Ocean. Environ. Sci. Technol. 41, 5608–5613.

Ding, X., Wang, X.-M., Xie, Z.-Q., Xiang, C.-H., Mai, B.-X., Sun, L.-G., Zheng, M., Sheng, G.-Y., Fu, J.-M., Pöschl, U., 2007. Atmospheric polycyclic aromatic hydrocarbons observed over the North Pacific Ocean and the Arctic area: spatial distribution and source identification. Atmos. Environ. 41, 2061–2072.

Ding, Y.H., 1994. The Summer Monsoon in East Asia, in: Monsoons over China. Springer, Netherlands, Dordrecht, pp. 1–90.

Fernández, P., Grimalt, J.O., Vilanova, R.M., 2002. Atmospheric gas-particle partitioning of polycyclic aromatic hydrocarbons in high mountain regions of Europe. Environ. Sci. Technol. 36, 1162–1168.

Finizio, A., Mackay, D., Bidleman, T., Harner, T., 1997. Octanol-air partition coefficient as a predictor of partitioning of semi-volatile organic chemicals to aerosols. Atmos. Environ. 31, 2289–2296.

Gigliotti, C.L., Brunciak, P.A., Dachs, J., Glenn, T.R., Nelson, E.D., Totten, L.A., Eisenreich, S.J., 2002. Air—water exchange of polycyclic aromatic hydrocarbons in the New York—New Jersey, USA, Harbor Estuary. Environ. Toxicol. Chem. 21, 235–244.

Gonzalez-Gaya, B., Fernandez-Pinos, M.-C., Morales, L., Mejanelle, L., Abad, E., Pina, B., Duarte, C.M., Jimenez, B., Dachs, J., 2016. High atmosphere-ocean exchange of semivolatile aromatic hydrocarbons. Nat. Geosci. 9, 438–442. http://dx.doi.org/10.1038/ngeo2714.

Guazzotti, S.A., Suess, D.T., Coffee, K.R., Quinn, P.K., Bates, T.S., Wisthaler, A., Hansel, A., Ball, W.P., Dickerson, R.R., Neusüß, C., Crutzen, P.J., Prather, K.A., 2003. Characterization of carbonaceous aerosols outflow from India and Arabia: biomass/biofuel burning and fossil fuel combustion. J. Geophys. Res. Atmos. 108 (108). http://dx.doi.org/10.1029/2002JD003277.

Gustafson, K.E., Dickhut, R.M., 1997. Particle/gas concentrations and distributions of PAHs in the atmosphere of southern Chesapeake Bay. Environ. Sci. Technol. 31, 140–147.

Harner, T., Bidleman, T.F., 1998. Octanol–air partition coefficient for describing particle/gas partitioning of aromatic compounds in urban air. Environ. Sci. Technol. 32, 1494–1502.

Hoffman, E.J., Mills, G.L., Latimer, J.S., Quinn, J.G., 1984. Urban runoff as a source of polycyclic aromatic hydrocarbons to coastal waters. Environ. Sci. Technol. 18, 580–587.

Jurado, E., Jaward, F.M., Lohmann, R., Jones, K.C., Simó, R., Dachs, J., 2004. Atmospheric dry deposition of persistent organic pollutants to the Atlantic and inferences for the global oceans. Environ. Sci. Technol. 38, 5505–5513.

Kawamura, K., Ishimura, Y., Yamazaki, K., 2003. Four years' observations of terrestrial lipid class compounds in marine aerosols from the western North Pacific. Glob. Biogeochem. Cycles 17, 3–19. http://dx.doi.org/10.1029/2001GB001810.

Kunwar, B., Kawamura, K., 2014. One-year observations of carbonaceous and nitrogenous components and major ions in the aerosols from subtropical Okinawa Island, an outflow region of Asian dusts. Atmos. Chem. Phys. 14, 1819–1836.

Kunwar, B., Kawamura, K., Zhu, C., 2016. Stable carbon and nitrogen isotopic compositions of ambient aerosols collected from Okinawa Island in the western North Pacific Rim, an outflow region of Asian dusts and pollutants. Atmos. Environ. 131, 243–253.

Kim, J.Y., Lee, J.Y., Choi, S.D., Kim, Y.P., Ghim, Y.S., 2012. Gaseous and particulate polycyclic aromatic hydrocarbons at the Gosan background site in East Asia. Atmos. Environ. 49, 311–319.

Lammel, G., Meixner, F.X., Vrana, B., Efstathiou, C.I., Kohoutek, J., Kukučka, P., Mulder, M.D., Přibylová, P., Prokeš, R., Rusina, T.P., Song, G.Z., Tsapakis, M., 2016. Bidirectional air–sea exchange and accumulation of POPs (PAHs, PCBs, OCPs and PBDEs) in the nocturnal marine boundary layer. Atmos. Chem. Phys. 16, 6381–6393.

Lei, Y.D., Chankalal, R., Chan, A., Wania, F., 2002. Supercooled liquid vapor pressures of the polycyclic aromatic hydrocarbons. J. Chem. Eng. Data 47, 801–806.

Lin, T., Hu, L., Guo, Z., Qin, Y., Yang, Z., Zhang, G., Zheng, M., 2011. Sources of polycyclic aromatic hydrocarbons to sediments of the bohai and yellow seas in East Asia. J. Geophys. Res. Atmos. 116, D23305. http://dx.doi.org/10.1029/2011JD015722.

Liu, H., Jacob, D.J., Bey, I., Yantosca, R.M., Duncan, B.N., Sachse, G.W., 2003. Transport pathways for Asian pollution outflow over the Pacific: interannual and seasonal variations. J. Geophys. Res. Atmos. 108, 8786. http://dx.doi.org/10.1029/2002JD003102.

Lohmann, R., Harner, T., Thomas, G.O., Jones, K.C., 2000. A comparative study of the gas-particle partitioning of PCDD/Fs, PCBs, and PAHs. Environ. Sci. Technol. 34, 4943–4951.

Lohmann, R., Klanova, J., Pribylova, P., Liskova, H., Yonis, S., Bollinger, K., 2013. PAHs on a west-to-east transect across the tropical Atlantic Ocean. Environ. Sci. Technol. 47, 2570–2578.

Lohmann, R., Lammel, G., 2004. Adsorptive and absorptive contributions to the gas-particle partitioning of polycyclic aromatic hydrocarbons: State of knowledge and recommended parameterization for modeling. Environ. Sci. Technol. 38, 3793–3803.

Ma, Y., Xie, Z., Yang, H., Möller, A., Halsall, C., Cai, M., Sturm, R., Ebinghaus, R., 2013. Deposition of polycyclic aromatic hydrocarbons in the north pacific and the arctic. J. Geophys. Res. Atmos. 118, 5822–5829. http://dx.doi.org/10.1002/jgrd.50473.

Matsui, H., Koike, M., Kondo, Y., Oshima, N., Moteki, N., Kanaya, Y., Takami, A., Irwin, M., 2013. Seasonal variations of Asian black carbon outflow to the Pacific: contribution from anthropogenic sources in China and biomass burning sources in Siberia and Southeast Asia. J. Geophys. Res. Atmos. 118, 9948–9967. http://dx.doi.org/10.1002/jgrd.50702.

Mulder, M.D., Heil, A., Kukučka, P., Klánová, J., Kuta, J., Prokeš, R., Sprovieri, F., Lammel, G., 2014. Air–sea exchange and gas–particle partitioning of polycyclic aromatic hydrocarbons in the Mediterranean. Atmos. Chem. Phys. 14, 8905–8915.

Nizzetto, L., Lohmann, R., Gioia, R., Jahnke, A., Temme, C., Dachs, J., Herckes, P., Guardo, Di, A., Jones, K.C., 2008. PAHs in air and seawater along a north–south Atlantic transect: trends, processes and possible sources. Environ. Sci. Technol. 42, 1580–1585.

Nizzetto, L., Macleod, M., Borgå, K., Cabrerizo, A., Dachs, J., Guardo, Di, A., Ghirardello, D., Hansen, K.M., Jarvis, A., Lindroth, A., Ludwig, B., Monteith, D., Perlinger, J.A., Scheringer, M., Schwendenmann, L., Semple, K.T., Wick, L.Y., Zhang, G., Jones, K.C., 2010. Past, present, and future controls on levels of persistent organic pollutants in the global environment. Environ. Sci. Technol. 44, 6526–6531.

Obata, A., Ishizaka, J., Endoh, M., 1996. Global verification of critical depth theory for phytoplankton bloom with climatological in situ temperature and satellite ocean color data. J. Geophys. Res. Ocean. 101, 20657–20667. http://dx.doi.org/10.1029/96JC01734.

Odabasi, M., Cetin, E., Sofuoglu, A., 2006. Determination of octanol–air partition coefficients and supercooled liquid vapor pressures of PAHs as a function of temperature: application to gas–particle partitioning in an urban atmosphere. Atmos. Environ. 40, 6615–6625.

Pankow, J.F., 1994. An absorption model of gas/particle partitioning of organic compounds in the atmosphere. Atmos. Environ. 28, 185–188.

Pankow, J.F., Bidleman, T.F., 1991. Effects of temperature, TSP and percent non-exchangeable material in determining the gas–particle partitioning of organic compounds. Atmos. Environ. Part a-General Top. 25, 2241–2249.

Ren, H., Kawagoe, T., Jia, H., Endo, H., Kitazawa, A., Goto, S., Hayashi, T., 2010. Continuous surface seawater surveillance on poly aromatic hydrocarbons (PAHs) and mutagenicity of East and South China Seas. Estuar. Coast. Shelf Sci. 86, 395–400.

Russo, R.S., Talbot, R.W., Dibb, J.E., Scheuer, E., Seid, G., Jordan, C.E., Fuelberg, H.E., Sachse, G.W., Avery, M.A., Vay, S.A., Blake, D.R., Blake, N.J., Atlas, E., Fried, A.,

Sandholm, S.T., Tan, D., Singh, H.B., Snow, J., Heikes, B.G., 2003. Chemical composition of Asian continental outflow over the western Pacific: results from transport and chemical evolution over the Pacific (TRACE-P). J. Geophys. Res. Atmos. 108, 8804. http://dx.doi.org/10.1029/2002JD003184.

Schwarzenbach, R.P., Gschwend, P.M., Imboden, D.M., 2003. Environmental Organic Chemistry, second ed. Wiley, Hoboken, USA, pp. 906–937.

Semeena, V.S., Lammel, G., 2005. The significance of the grasshopper effect on the atmospheric distribution of persistent organic substances. Geophys. Res. Lett. 32, L07804. http://dx.doi.org/10.1029/2004GL022229.

Simcik, M.F., Franz, T.P., Zhang, H., Eisenreich, S.J., 1998. Gas-particle partitioning of PCBs and PAHs in the Chicago urban and adjacent coastal atmosphere: States of equilibrium. Environ. Sci. Technol. 32, 251–257.

Tang, Y., Carmichael, G.R., Seinfeld, J.H., Dabdub, D., Weber, R.J., Huebert, B., Clarke, A.D., Guazzotti, S.A., Sodeman, D.A., Prather, K.A., Uno, I., Woo, J.-H., Yienger, J.J., Streets, D.G., Quinn, P.K., Johnson, J.E., Song, C.-H., Grassian, V.H., Sandu, A., Talbot, R.W., Dibb, J.E., 2004. Three-dimensional simulations of inorganic aerosol distributions in East Asia during spring 2001. J. Geophys. Res. Atmos. 109, D19S23. http://dx.doi.org/10.1029/2003JD004201.

Verma, S.K., Kawamura, K., Chen, J., Fu, P., Zhu, C., 2015. Thirteen years of observations on biomass burning organic tracers over Chichijima Island in the western North Pacific: an outflow region of Asian aerosols. J. Geophys. Res. Atmos. 120, 4155–4168.

Wang, F., Lin, T., Li, Y., Ji, T., Ma, C., Guo, Z., 2014. Sources of polycyclic aromatic hydrocarbons in PM2.5 over the East China Sea, a downwind domain of East Asian continental outflow. Atmos. Environ. 92, 484–492.

Wania, F., Mackay, D., 1993. Global fractionation and cold condensation of low volatility organochlorine compounds in Polar Regions. Ambio 22, 10–18.

Xu, Y., Zhang, Y.-L., Li, J., Gioia, R., Zhang, G., Li, X.-D., Spiro, B., Bhatia, R.S., Jones, K.C., 2012. The spatial distribution and potential sources of polycyclic aromatic hydrocarbons (PAHs) over the Asian marginal seas and the Indian and Atlantic Oceans. J. Geophys. Res. Atmos. 117, D07302. http://dx.doi.org/10.1029/2011JD016585.